Tuning the Catalytic Properties of UiO-66 Metal-Organic Frameworks: From Lewis to Defect-induced Brønsted Acidity

F. G. Cirujano[a,b,*] and F. X. Llabrés i Xamena[a,*]

[a] *Instituto de Tecnología Química, Universitat Politècnica de València, Consejo Superior de Investigaciones Científicas, Avda. de los Naranjos, s/n, 46022 Valencia, Spain.*

[b] *Current address: Instituto de Ciencia Molecular (ICMOL), Universitat de Valencia, Catedrático José Beltrán Martínez nº 2, 46980 Paterna, Valencia, Spain.*

Abstract

Lewis/Brønsted acidity and catalytic properties of UiO-66-type metal-organic frameworks are studied as tunable acid catalysts based on the presence of linker defects that create coordinatively unsaturated Zr^{4+} centers. FTIR spectroscopy of adsorbed CO and direct pH measurements are employed to characterize hydrated and dehydrated UiO-66 containing different number of Zr^{4+} sites associated with defects. These sites can strongly polarize coordinated water molecules, which induces Brønsted acidity in the hydrated material. Upon dehydration of the solid, the coordinated water molecules are removed, and the underlying coordinatively unsaturated Zr^{4+} cations become exposed and available as Lewis acid sites. Herein we show, for various acid catalyzed reactions, how it is possible to shift from a Brønsted acid to a Lewis acid catalyst by simply controlling the hydration degree of the solid. This control adds a new dimension to the design and engineering of MOFs for catalytic applications.

TOC image

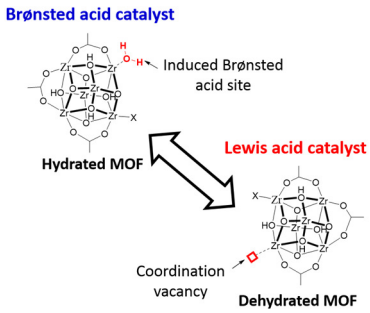

Metal-Organic Frameworks (MOFs) have received a great deal of attention in heterogeneous catalysis due to their high tunability of pore structure and chemical composition.[1-5]. This can be achieved by properly selecting the structural components forming the MOF (metal and organic ligands) from an almost infinite number of possibilities, and by using post-synthesis modification strategies to introduce new functionalities.[6-8] Moreover, the crystalline nature of these compounds allows us, in principle, to predict the acid[9-10] and basic[11-12] properties of MOFs with theoretical calculations based on model clusters taken from the ideal crystalline network and to establish structure-activity relationships. However, in real MOFs, the regular framework is interrupted by the (un)intentional occurrence of point defects, which can change abruptly the catalytic and adsorption properties compared to those predicted for the ideal compound. Nonetheless, the presence of defects in MOF lattices does not necessarily imply a depletion of the properties of the material, but they can bring about new types of centers that can improve catalytic performance, or even introduce new functionalities that are absent in the defect-free parent solid.[13] For instance, in the ideal lattice of zirconium-containing UiO-66-type MOFs, Zr ions are completely saturated by the organic ligands. However, Zr^{4+} coordination vacancies are created during the synthesis of UiOs associated with missing linkers. As a result, while ideal UiO-66 should not have acid properties, the real (defective) materials display the typical reactivity of a solid acid, and are active in several reactions, including esterification of carboxylic acids,[14-15] Diel-Alder condensation,[16] CO_2 cycloaddition to epoxides,[17] cross-aldol condensation,[18] carbonyl-ene isomerization of citronellal to isopulegol,[9] Meerwein-Ponndorf-Verley reduction of carbonyl compounds,[19-20] etc. Moreover, the catalytic activity of defective UiOs gradually increases with the concentration of defects in the structure.[15, 19, 21]

To gain further insights into the nature of these defects under different hydration conditions and their role in the observed catalytic activity, we have now rationalized the properties of various UiOs bearing different functionalities at the organic linkers and having different numbers of defects.[22] Herein we will show that Zr^{4+} defects associated with missing linkers of hydrated UiOs can strongly activate water molecules, thus behaving as typical Brønsted acid catalysts. Meanwhile, these coordinated water molecules are removed upon thermal dehydration of the solid, and the underlying Zr^{4+} sites remain exposed and available as Lewis acid centers. We will thus demonstrate that it is possible to shift from a Lewis acid to a Brønsted acid catalyst by simply controlling the hydration degree of the solid, which adds a new dimension to the design and

engineering of MOFs for catalytic applications (acidity on demand). This process is depicted in Scheme 1.

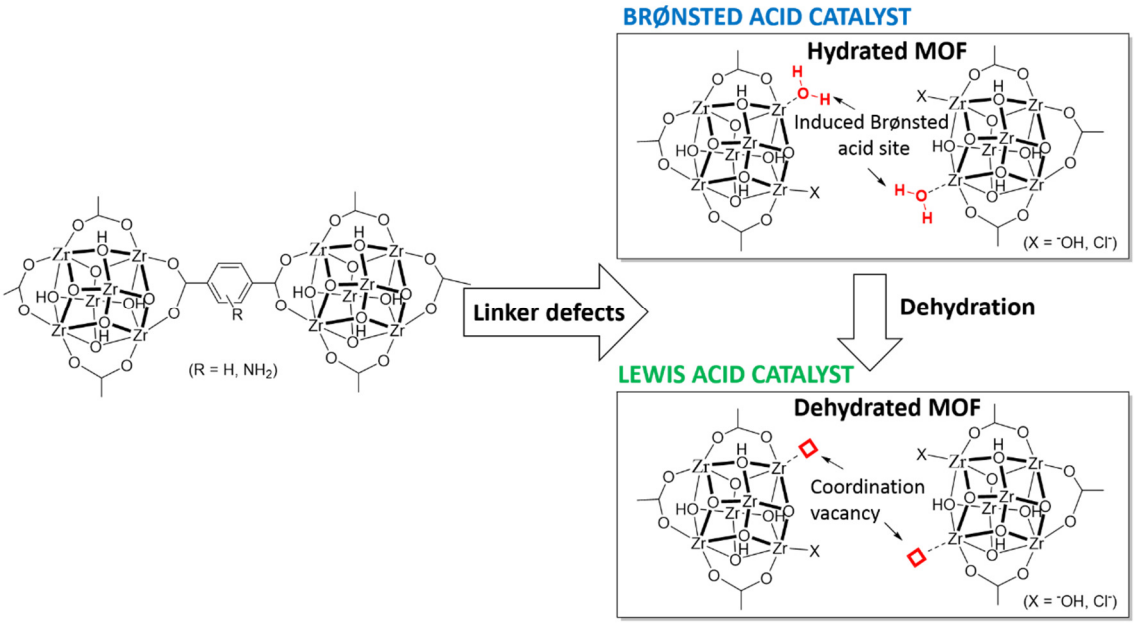

Scheme 1. Linker deficiencies (point defects) in hydrated and dehydrated UiO-66 type compounds.

Suitable catalytic test reactions have been selected to evaluate the properties of defective UiOs as either Brønsted or Lewis acid solids. On the one hand, esterification of levulinic acid is used to evaluate Brønsted acidity. Indeed, the importance of Brønsted acid sites for esterification reactions has been highlighted for micro/mesoporous zeolites,[23] heteropolyacids,[24] sulfated oxides[25] or acid impregnated clays.[26] In the case of MOFs, Goesten et al.[27] and Jiang et al.[28] showed that upon treatment with sulfuric acid, chemically stable MOF structures Cr-MIL-101 or Zr-MOF-88 can be sulfated, resulting in Brønsted acid sulfate groups attached to the terephthalate linkers with remarkable catalytic activity for the esterification of carboxylic acids. On the other side of the scale, several reactions require Lewis instead of Brønsted acid centers as the catalytic active sites. Examples of such reactions are citronellal isomerization to isopulegol through an intramolecular carbonyl-ene reaction, as well as the Meerwein-Ponndorf-Verley (MPV) reduction of carbonyl compounds with secondary alcohols. Both of them can be considered as model reactions to monitor the Lewis acid site concentration, availability, and strength of a solid catalyst. Moreover, both reactions can be catalyzed by UiO-66, as well as other MOFs containing zirconium[20, 28-29] or other metal cations.[29-31]

Previous results

We will start the current discussion by reviewing the data available from previous studies on UiOs. Figure 1 summarizes the main results obtained so far.

The catalytic activity of UiOs for the esterification of carboxylic acids increases with the number of defects of the solid (see Fig. 1a)[15] and decreases significantly upon dehydration of the solid[32]. Thus, adsorbed water is beneficial for this reaction (Fig. 1b). *Ab initio* calculations confirmed that the energy barriers for the esterification reaction are considerably higher for a dehydrated defect that for a hydrated acid site. A dual Lewis/Brønsted catalytic mechanism was then proposed, which is more efficient in the hydrated solid than in the dehydrated material (Fig. 1c)[32].

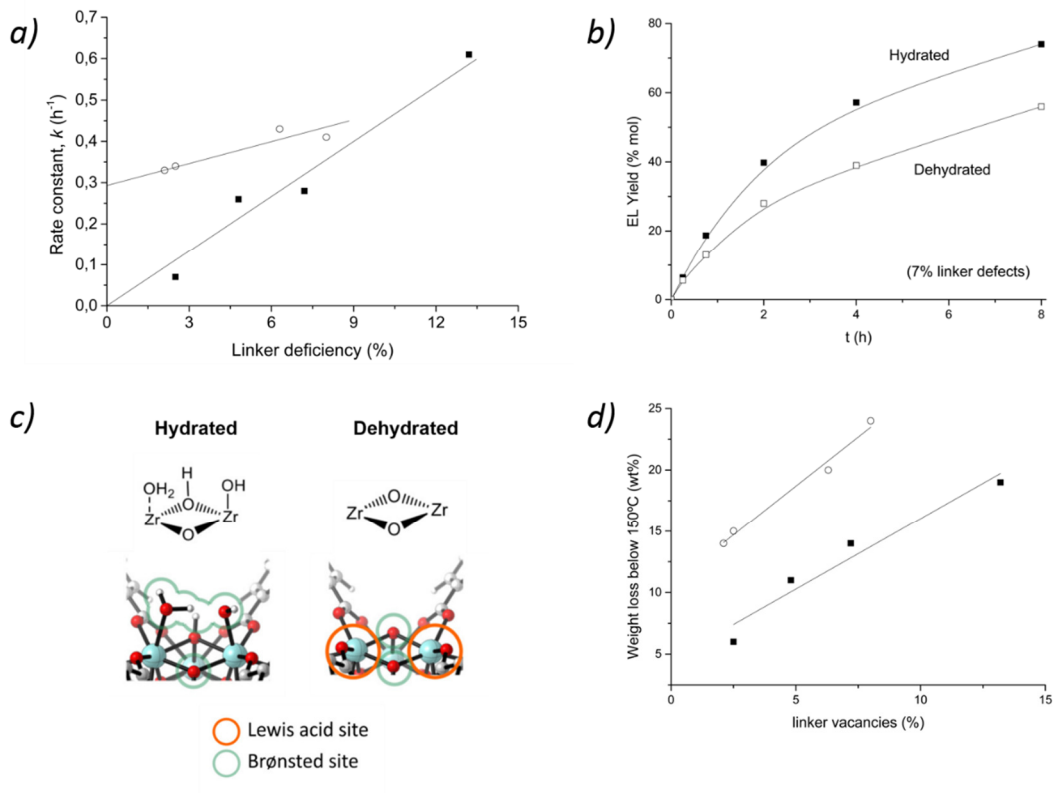

Figure 1. Most relevant conclusions extracted from previous works on UiO-66. *a*) Dependency of the rate constant levulinic acid esterification with ethanol on the number of linker defects in UiO-66 (-■-) and UiO-66-NH_2 (-○-) [15]; *b*) Kinetic data of levulinic acid esterification over hydrated and dehydrated UiO-66 [32]; c) Proposed active sites on hydrated and dehydrated UiO-66 [32]; and d) Dependency of the amount of physisorbed water on the number of linker defects in UiO-66 (-■-) and UiO-66-NH_2 (-○-) [32].

Linker defects also increase the total amount and adsorption strength of physisorbed water of the solid surface (Fig. 1d)[32]. This was already predicted theoretically

by Snurr and co-workers[33], and confirmed experimentally by Fischer and co-workers[21]. Thus, the higher hydrophilicity of defective UiOs compared to defect-free compounds was assumed to be the major reason for the higher catalytic activity of defective UiOs. Significant differences were also observed between UiO-66 and UiO-66-NH_2 materials (i.e., a material isoreticular to UiO-66 but bearing amino groups in the terephthalate linkers), being UiO-66-NH_2 samples slightly more active for esterification than the UiO-66 with the same number of linker defects (Fig. 1a). Also, the total amount of physisorbed water in UiO-66-NH_2 was higher than in UiO-66 with a similar concentration of linker defects, and water molecules were more strongly bound (Fig. 1d). Therefore, the presence of amino groups favors water adsorption, in line with previous results by Walton and co-workers [34]. Even though our theoretical models did not predict a direct participation of the amino groups in any of the steps of the esterification reaction, their presence increases the amount of water adsorbed by the solid compared to UiO-66.

In summary, the number of linker defects, the hydration state of the solid and the presence or not of amino groups (or other functional groups) in the terephthalate linkers determine the environment inside the cavities of UiOs, and will all have a large impact on the catalytic properties of the final material.

In line with the results commented above, it is now convenient to analyze the differential characteristics of hydrated and dehydrated UiO compounds (both UiO-66 and UiO-66-NH_2) and containing different concentrations of linker defects, with special emphasis on determining the Brønsted acidity of the materials. We will then explore how this knowledge can assist in tuning the catalytic properties of the material to optimize its performance in specific reactions.

Brønsted-induced acidity in defective UiO-66

FTIR spectroscopy of adsorbed CO

Low-temperature FTIR spectroscopy of adsorbed CO is a widely used technique to monitor the type (Brønsted and Lewis), concentration and strength of the acid sites on the surface of a solid catalyst[35-37]. To analyze the influence of the defect content on the CO adsorption properties of UiO-66, the measurements have been performed onto two samples containing either a low (2%) or a high (7%) amount of linker defects. Further information on these samples is given in the Experimental details below. Likewise, the effect of the hydration degree of the catalyst has been addressed by selecting two thermal

activation conditions, 60ºC or 200ºC under vacuum for 6 hours. Note that thermal activation at 60ºC is enough to remove only loosely bound (physisorbed) water molecules inside the pores, but not tightly coordinated water molecules (see below).

Figure 2 shows the infrared spectra obtained before and after the adsorption of CO. Both, the number of defects of the sample and the activation procedure used before CO adsorption have a large impact on the corresponding FTIR spectra. Thus, when the samples were fully dehydrated (activated at 200ºC, *top* and *middle* parts of Figure 2), the spectra before CO adsorption present mainly a single absorption band at 3674 cm^{-1}, which has been previously attributed to the O-H stretching mode of isolated hydroxyl groups at the triangular faces of the $[Zr_6(OH)_4O_4]$ inorganic building units, i.e. μ_3-OH groups [38]. Note that these μ_3-OH are only removed at temperatures above 300ºC. For the sample with 7% missing linkers, additional (minor) bands are also observed at 3689, 3657 and 3610 cm^{-1}, which are assigned to O-H stretching modes of different hydroxylated species, as described in detail in reference [39] and whose in-depth discussion is beyond the scope of this work.

Upon CO adsorption, the bands at 3674 cm^{-1} in both samples are completely eroded due to the formation of hydrogen-bonded adducts between CO and the μ_3-OH groups of the solid. These H-bonded adducts are responsible for the new (broader) band centered at 3600 cm^{-1} ($\Delta\nu$(O-H) = -74 cm^{-1}), while the corresponding C-O stretching mode is observed at 2153-2154 cm^{-1}. These values of $\Delta\nu$(O-H) are typical of very weak acid sites and are in line with previous studies on CO adsorption onto UiO-66 materials [40-43]. In the C-O region of the spectra, besides the main band at 2154 cm^{-1} already mentioned, an additional absorption is observed at 2178 cm^{-1} (shifting to 2173 cm^{-1} at high CO doses) for the highly defective UiO-66 sample. This band reflects the existence of coordinatively unsaturated (*cus*) Zr^{4+} ions acting as Lewis acid sites. Note that this band is also present in the less defective sample (see inset) although with a much lower relative intensity than in the more defective material. These results indicate that the amount of Lewis acid sites in UiO-66 increases with the concentration of linker defects of the solid, as expected. We will see in the following that this has a large impact on the catalytic properties of the fully dehydrated materials (i.e., activated at 200ºC under vacuum) as Lewis acid catalysts. Finally, another C-O band at 2137 cm^{-1} is observed for the highest CO doses that correspond to physisorbed CO inside the MOF pores. Scheme 2 summarizes the main species and corresponding IR band assignments.

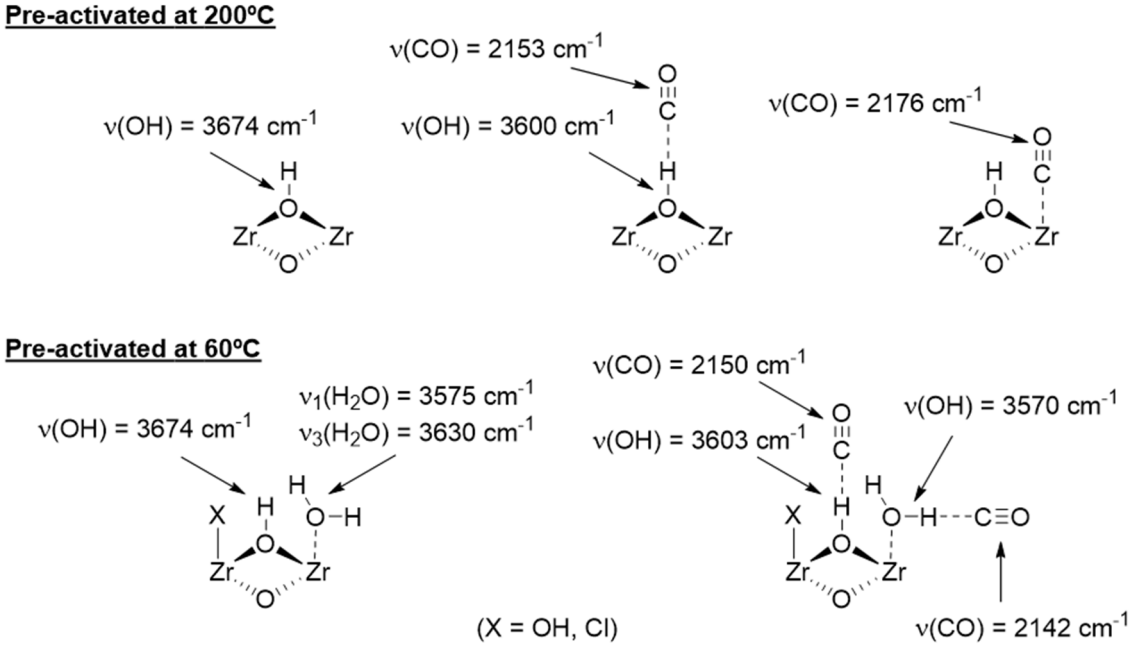

Scheme 2. Main FTIR characteristics of CO adsorbed on UiO-66.

On the other hand, the IR spectrum of a partially hydrated sample (activated at 60ºC) shows significant differences compared to fully dehydrated samples. In the spectrum before CO adsorption, main IR absorptions appear now at 3674 cm^{-1}, 3630 cm^{-1}, and 3575 cm^{-1}; the latter two being absent in the spectra of fully dehydrated samples. Adsorption of CO produces a significant (although not complete) erosion of the bands at 3674 cm^{-1} and 3630 cm^{-1}, while new bands develop at 3603 cm^{-1} and 3570 cm^{-1}. The fate of the band at 3575 cm^{-1} is not clear since it is overshadowed by the new bands appearing after CO adsorption. In the C-O stretching region, two IR absorption bands develop at 2150 and 2142 cm^{-1}, together with a shoulder at ~2135 cm^{-1} (due to physisorbed CO). Note that the ν(CO) band that was observed at 2178 cm^{-1} for the sample activated at 200ºC is not present in the sample activated at 60ºC (see inset in Figure 2). This means that Lewis acid sites are barely present in partially dehydrated samples.

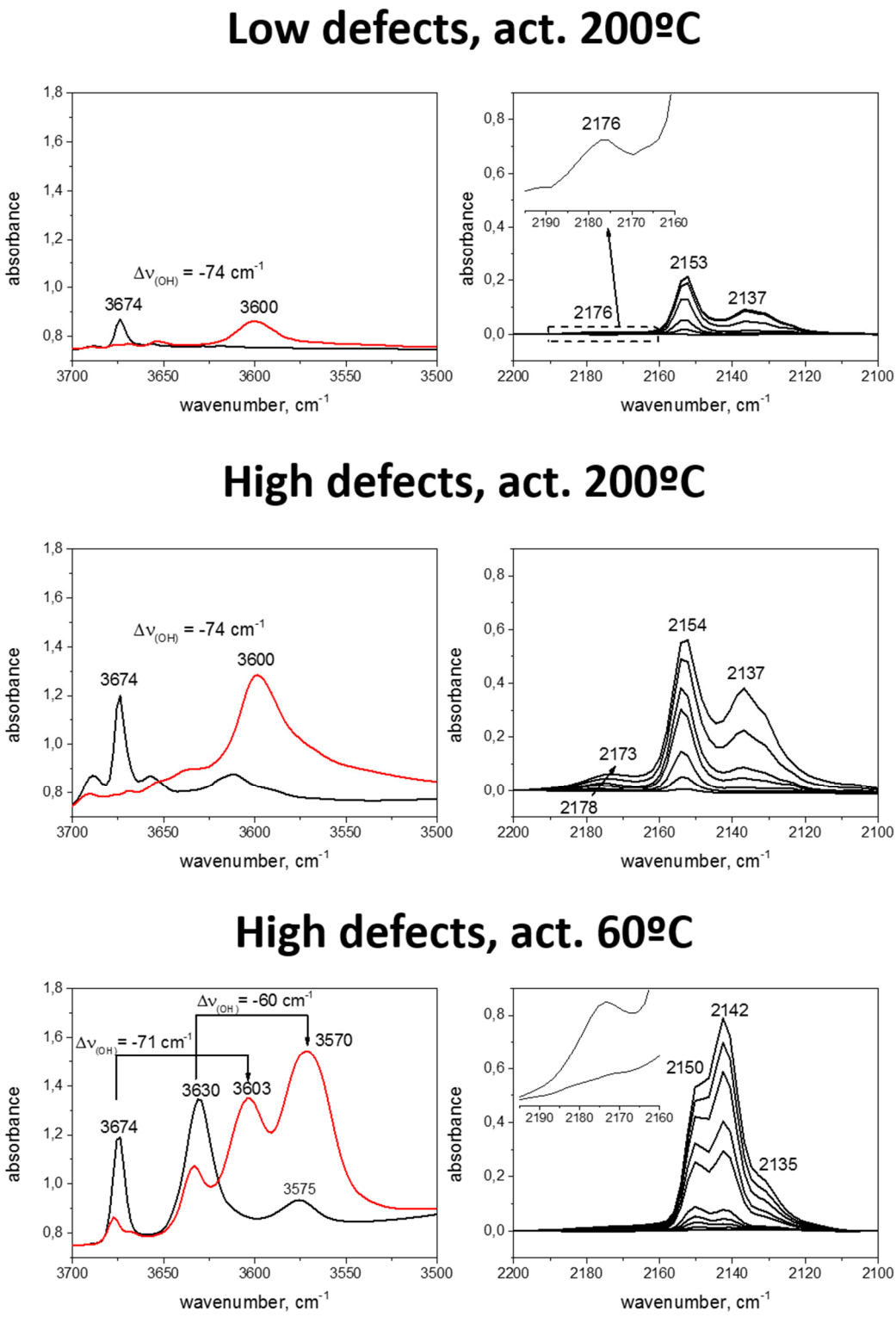

Figure 2. FTIR spectra of CO adsorbed (at 77 K) on UiO-66: (*Top*) UiO-66 with 2% of linker defects, pre-activated at 200ºC before (black curve) and after (red curve) CO adsorption; (*Middle*) UiO-66 with 7% of linker defects, pre-activated at 200ºC; and (*Bottom*) UiO-66 with 7% of linker defects, pre-activated at 60ºC. The inset in the bottom-right plot compares the band at 2176 cm-1 for the sample with 7% of defects pre-activated at 200ºC and 60ºC. All spectra have been normalized to the amount of Zr in each sample.

Referring to the spectra of samples activated at high temperature commented above, it should be clear that the bands at 3674 cm^{-1} and 3603 cm^{-1} can readily be attributed to isolated μ_3-OH groups and μ_3-OH···CO H-bonded adducts, respectively, while the corresponding C-O band of these H-bonded adducts is observed now at 2150 cm^{-1}. Once these bands are assigned, we attribute the remaining absorption bands at 3630 and 3575 cm^{-1} to the ν_3 and ν_1 O-H stretching modes of water molecules coordinated to Zr^{4+} ions, respectively. Meanwhile, the bands at 3570 cm^{-1} and 2142 cm^{-1} formed after CO adsorption should correspond respectively to the $\nu_{(OH)}$ and $\nu_{(C-O)}$ modes of H-bonded adducts of coordinated water molecules with CO. This assignment is supported by previous studies on CO adsorption onto a Cr- and Al-containing MIL-100 MOF, in which similar bands were observed and were analogously attributed to water molecules coordinated to Cr^{3+} *cus* of the material interacting with CO.[44-46] However, there are clear differences in the type of *cus* present in these two materials, viz. Cr^{3+} or Al^{3+} in MIL-100 and Zr^{4+} in UiO-66. The crystalline network of MIL-100 contains "intrinsic" *cus*; i.e., trinuclear $M_3(\mu_3\text{-O})$ ($M = Cr^{3+}$, Al^{3+}) units in which two of the M^{3+} ions are coordinated to labile H_2O molecules on apical positions. There is a 2:3 stoichiometric amount of coordinated water molecules and M^{3+} sites in the material. On the contrary, in the ideal structure of UiO-66, the Zr^{4+} ions are (in principle) completely blocked by the carboxylate ligands. Therefore, coordination of H_2O molecules is only possible at defective positions associated to linker vacancies. Thus, the number of coordinated water molecules can largely vary from sample to sample, depending on the number of linker defects. In this way, the higher the number of linker defects of UiO-66, the higher the amount of coordinated H_2O molecules can be expected.

Note that the coordination of a water molecule to the metal cation of the MOF increases the Brønsted acidity of this molecule; i.e., the O-H bond of H_2O is weakened [47]. Therefore, we can consider a Brønsted-induced acidity of UiO-66 materials upon water coordination to Zr^{4+} at defect sites, as we will show below. Janiak and co-workers also reached a similar conclusion when studying various Cr^{3+}-containing MIL-101 materials and also attributed a Brønsted-induced acidity to the materials upon water adsorption on the Cr^{3+} *cus* [48]. More recently, Yaghi and co-workers used a combination of spectroscopic and theoretical tools and concluded that coordinated water molecules were the strongest Brønsted acid sites of sulfated MOF-808 and that the material loosed its acidity on dehydration [49] (as evidenced by the lower catalytic activity of dehydrated MOF-808-SO_4

in isobutene dimerization compared to the hydrated material). As we have shown here using FTIR spectroscopy of adsorbed CO, the amount of such Brønsted-induced acid sites in UiO-66 (responsible for the band at 3630 cm^{-1}) increases with the number of linker defects, but they are only present in partially hydrated samples. When the solid is degassed at a temperature above 150ºC, coordinated water molecules are removed and the Brønsted acidity is lost, in line with the results on MOF-808-SO_4 commented above [49]. As a consequence, the Zr^{4+} ions that were formerly blocked by H_2O molecules become now accessible for adsorption, resulting in the creation of Lewis acid sites (evidenced by the band at 2178 cm^{-1} upon CO adsorption). Thus, these results indicate that it should be possible to tune the acid properties of UiO-66, moving from a Brønsted-induced acid to a Lewis acid catalyst, by simply controlling the hydration degree of the material through appropriate thermal treatments. Moreover, the linker vacancies increase both, the amount of Brønsted acid sites in the hydrated material, and the amount of Lewis acid sites in the dehydrated material. We will show below that this can be efficiently exploited to optimize the catalytic properties of the material for reactions requiring either Brønsted or Lewis acid catalytic sites.

Another important difference between UiO-66 and Cr-MIL-100 or Cr-MIL-101 materials commented above [45, 48] is the polarizability (or hardness) of the metal ions of the MOF. The polarizing power (Z^2/r) of the metal cation is much higher for Zr^{4+} than for Cr^{3+}: 18.6 vs. 11.9 (with r in angstroms), respectively. Indeed, Cr^{3+} is considered a moderately acidic cation (the pK_a of the metal aquo complex is 4), while Zr^{4+} is strongly acidic (pK_a = -0.3) [50]. Nevertheless, the effective Brønsted acidity of the adsorbed water molecules will depend not only on the polarizing power of the metal cation present in the MOF (e.g., Zr^{4+} or Cr^{3+}) but also on the type of ligands and coordination environment imposed by the MOF structure.

pH measurements

The Brønsted acid properties of a material can also be evidenced by measuring the pH change of a solvent upon immersing the solid inside[51]. These studies are usually carried out by potentiometric acid-base titrations, in which a small amount of the solid is dispersed in an aqueous solution of a suitable electrolyte, such as $NaNO_3$ or NaCl, and allowed to equilibrate for several hours before the measurement. In this way, Farha and co-workers used potentiometric titration to evaluate the Brønsted of a number of water stable Zr_6- and Hf_6-based MOFs, including UiOs, NU-1000, and MOF-808[52]. For each

compound, pK_a values were determined for the three typical types of protons: μ_3-OH, M–OH_2, and M–OH (M = Zr, Hf). In the particular case of UiO-66, the pK_a values found were 3.52±0.02, 6.79±0.01 and 8.30±0.02, respectively.

Since the above potentiometric titration measurements were carried out in aqueous media, it is evident that the same method cannot be used if we want to analyze the dependence of the hydration degree of the UiO-66 materials on their acidity. As an alternative, methanol can be chosen as a solvent instead of water, following the method used in reference [48]. Table 1 shows the pH values measured for stirred suspensions of various MOFs in methanol.

As it can be seen in Table 1, a suspension of hydrated UiO-66 MOFs in methanol lowers the pH of the solvent, and the effect is more marked when the amount of linker defects of the MOF increases: 2.5 and 3.7 for samples containing 7% and 2% of missing linkers, respectively (compare entries 2 and 5). In agreement with previous observations [48], when the solid is removed by filtration or centrifugation, the pH of the filtrate is virtually unchanged compared to free methanol (see entry 3), which shows that the Brønsted-induced acidity of UiO-66 is a surface effect; i.e., the pH of the solvent is only lowered in the vicinity of the solid. On the other hand, fully dehydrated UiO-66 produces a much less pronounced pH decrease than hydrated MOF: 3.2 vs, 2.5 (entries 2 and 4), and 3.7 vs. 5.8 (entries 5 and 6) for samples with 7% and 2% defects, respectively. These results reinforce our above interpretation of the IR results and the occurrence of a Brønsted-induced acidity of UiO-66 as a consequence of water coordination to the Zr^{4+} sites associated with linker defects. Nonetheless, the pH measured for dehydrated UiO-66 is still lower than that of pure methanol: 3.2 and 5.8 for dehydrated UiO-66 with 7% and 2% defects, respectively (entries 4 and 6), with respect to 6.0 for pure methanol. Since adsorbed water is no longer present in these samples, the measured decrease of the pH value reflects the polarizing power of the Zr^{4+} sites of the MOF on the methanol molecules. Indeed, Vimont et al. showed that unsaturated Cr^{3+} ions in MIL-100 were also able to strongly adsorb and polarize a number of alcohols (including methanol), thus inducing Brønsted acid sites whose strength depends on the adsorbate.[45]

Table 1. pH values of stirred suspensions of various MOFs in methanol.[a]

Entry	Catalyst	% missing linkers	pH
1	Blank (methanol alone)	-	6.0
2	Hydrated UiO-66	7	2.5
3	Filtrate of hydrated UiO-66 [b]	7	5.8
4	DehydratedUiO-66 [c]	7	3.2
5	Hydrated UiO-66	2	3.7
6	Dehydrated UiO-66	2	5.8
7	Hydrated UiO-66-NH_2	8.8	1.6
8	DehydratedUiO-66-NH_2 [c]	8.8	2.2
9	Hydrated UiO-66-NO_2	0.1	3.5
10	Dehydrated UiO-66-NO_2 [c]	0.1	4.9
11	Hydrated UiO-66-HAc	-	5.6
12	Hydrated UiO-66-SO_3H	-	3.6
13	Dehydrated UiO-66-SO_3H	-	3.8

[a] pH of a stirred suspension of 6 mg of MOF in 24 mL of methanol, 25ºC. [b] pH of the filtrate of suspension of entry 2. [c] The MOF was dried 6 h at 200ºC under vacuum before preparing the suspension in methanol.

To determine if this trend was also observed in other MOFs, we performed similar pH measurements on UiO-66-NH_2 and UiO-66-NO_2 samples, both in their hydrated and dehydrated forms, and the results are also reported in Table 1. As it can be seen, also in this case the samples produce a more pronounced lowering of the pH for the hydrated than for the dehydrated solids. It is interesting to note that the sample UiO-66-NO_2 contains a much lower concentration of defects than the less defective UiO-66 (0.1% versus 2%, respectively), and yet the pH decrease observed with the nitro-containing MOF is slightly higher: 3.5 versus 3.7 (compare entries 5 and 9). This result reflects the electron-withdrawing effect of the nitro group in the terephthalate linker, making the Zr^{4+} ions in UiO-66-NO_2 more electropositive and therefore increasing their net effective charge. This translates into a higher effective polarizing power (Z^2/r ratio) of the Zr^{4+} ions in UiO-66-NO_2 and, thus, into a higher activation of the coordinated water molecules. This is in agreement with the observation that dehydrated UiO-66-NO_2 contains stronger Lewis acid sites than UiO-66, as revealed by FTIR spectroscopy of adsorbed 5-nonanone [12], and also indirectly evidenced by the higher catalytic activity of this compound compared to UiO-66 in Lewis acid-catalyzed reactions [9, 12].

To complete this picture of comparative pH measurements, we included a UiO-66 sample prepared with acetic acid as a modulator (UiO-66-HAc in Table 1). It is known that the acetic acid used in the synthesis remains strongly coordinated to the Zr^{4+} defective sites [19], thus blocking the sites and avoiding the induction of Brønsted acidity by water coordination. Accordingly, it was observed that the pH of a methanolic suspension of the sample UiO-66-HAc is very close to that of pure methanol (entry 11). Finally, we also considered a UiO-66-SO_3H sample. In this case, it was not possible to prepare this material by a two-step synthesis procedure similar to that used for the other compounds, and it was necessary to use acetic acid as a modulator to obtain a highly crystalline material. Considering the blocking effect of the acetic acid modulator, we believe that the Brønsted acidity of UiO-66-SO_3H, responsible for the observed pH lowering to 3.6, is mostly due to the sulfonic groups in the linkers rather than strongly coordinated water molecules (as in UiO-66, UiO-66-NH_2, and UiO-66-NO_2). In agreement with this assumption, we observed practically no variations of the pH when UiO-66-SO_3H was fully dehydrated (entries 12 and 13).

UiO-66 as a Brønsted-induced acid catalyst: Esterification of carboxylic acids

At the light of the Brønsted-induced acidity of UiO-66 type MOFs discussed above, we have now reexamined the esterification of levulinic acid with ethanol as a model reaction to investigate in more detail the effect of both, the number of linker defects and degree of hydration of the MOFs on their catalytic performance.

As we have discussed above, as the amount of linker defects in UiO-66 increases, the catalytic activity of the material for the esterification of LA also increases, following a clear linear trend (see Fig. 1a) [15]. Moreover, it is also observed that the dehydration of the samples by thermal treatment at 150ºC (see Fig. 1b) brings about a definite decrease in the catalytic activity of UiO-66 samples [32].

Therefore, it is evident that there is a clear interdependence of the number of linker defects and the hydration degree of the sample on one side, and the measured pH in methanol and catalytic activity for esterification (k) on the other side. This correlation can be easily evidenced by plotting the logarithm of the rate constant of esterification, log k, versus the pH measured upon dispersing the catalyst in methanol, as shown in Figure 3. In this plot, we have included all the MOF samples studied, as well as other Zr- and Hf-containing DUT-67 compounds [29] and other reference acid catalysts; viz., *para*-toluene sulfonic acid (*p*-TSA) and Amberlyst-15®. The strong correlation between the reaction

rate constant and the drop of the pH of methanol produced by the catalyst lend support to the hypothesis that the Brønsted-induced acid sites of the MOF are the most likely active sites for the esterification of LA. Meanwhile, the participation of Lewis acid sites of the solid (if any) must be very limited for this typical Brønsted acid catalytic reaction.

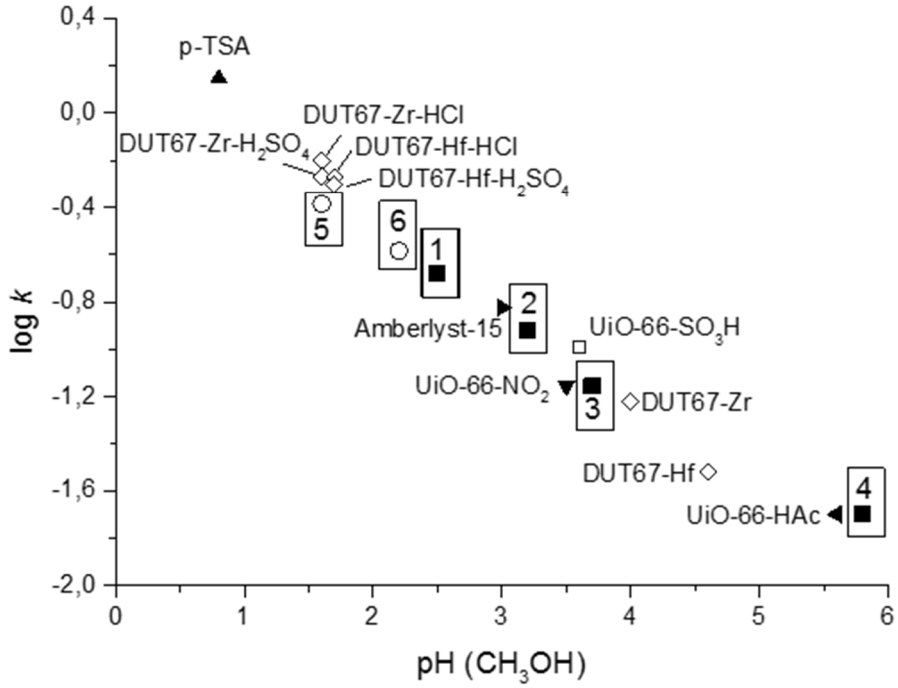

Figure 3. Logarithmic plot of the reaction rate constant of LA esterification (log *k*) versus the pH of a methanol dispersion of various catalysts, as indicated: *para*-toluene sulfonic acid (▲); Amberlyst-15® (►); UiO-66-NO_2 (▼); UiO-66-HAc (◄); UiO-66-SO_3H (□); various Zr- and Hf-DUT-67 (◊). Samples of UiO-66 (■) and UiO-66-NH_2 (○) are numbered as follows. 1) Hydrated UiO-66 (7% of defects); 2) Dehydrated UiO-66 (7% of defects); 3) Hydrated UiO-66 (2% of defects); 4) Dehydrated UiO-66 (2% of defects); 5) Hydrated UiO-66-NH_2 (8.8% of defects); 6) Dehydrated UiO-66-NH_2 (8.8% of defects).

In line with the above results, it has been described that interlamellar water molecules coordinated to aluminum ions of Al-exchanged montmorillonite (Al-Mont) provide strong Brønsted acid sites to catalyze the esterification of phenylacetic acid with *p*-cresol, while the parent Na-exchanged montmorillonite was not acidic (and therefore catalytically inactive) due to the low polarizing power of Na^+ as compared to Al^{3+} cations [53]. Thus, 67% conversion was attained over hydrated Al-Mont (solid dried at 100ºC), while the catalytic activity almost halved (36% conversion) when the solid was dried at 200ºC, and it was completely lost when dried at 400ºC. Therefore, the catalytic activity

of the clay mirrored the hydration degree of the solid, similar to what we have observed here for Zr UiO-66-type MOFs.

Taking together all the results discussed above, it can be concluded that dehydration of the UiO-66 samples produces a desorption of water molecules strongly coordinated to defective Zr^{4+}, as evidenced by the disappearance (see Fig. 2) of the IR absorption band at 3670 cm^{-1}. As a result, the Brønsted induced acidity of the MOF is lost, and therefore, the pH drop of methanol upon dispersing the dehydrated solid is less pronounced (see Table 1) than in the case of the hydrated sample. In turn, dehydration and loss of the Brønsted-induced acidity cause a decrease in the catalytic activity of the MOF for the esterification of LA. And these effects are more pronounced for the samples containing a higher concentration of missing linker defects.

UiO-66 as a Lewis acid: Citronellal isomerization and Meerwein-Ponndorf-Verley reduction of cyclohexanone.

Isomerization of citronellal (**1**) produces a mixture of isopulegol diastereoisomers, namely isopulegol, neo-isopulegol, iso-isopulegol and neoiso-isopulegol (**2**-**5**, Scheme 3). One of these products, isopulegol (**2**), can be further converted into the industrially relevant product menthol through hydrogenation of the terminal C=C bond. When a Lewis acid catalyst is used for the isomerization reaction, high selectivities are usually obtained to the desired isopulegol. However, with Brønsted acid catalysts, isopulegol is still the major product of this reaction, but it is obtained with significantly lower diastereoselectivities. This trend was nicely shown by Yaghi and co-workers when studying the catalytic activity of as-prepared and sulfated MOF-808, a zirconium trimesate compound [28]. Those authors observed a very low activity of as-prepared MOF-808 for citronellal isomerization (8% conversion after 8 h of reaction), albeit with a high selectivity to **2** (85%). Progressive sulfation of MOF-808 increased its Brønsted acidity and accelerated the conversion rate of citronellal (98% conversion after 1.5 h for the most sulfated compound), but the selectivity to **2** dropped progressively down to 55%, reflecting the increased participation of the newly introduced Brønsted acid sites in the catalytic conversion of citronellal.

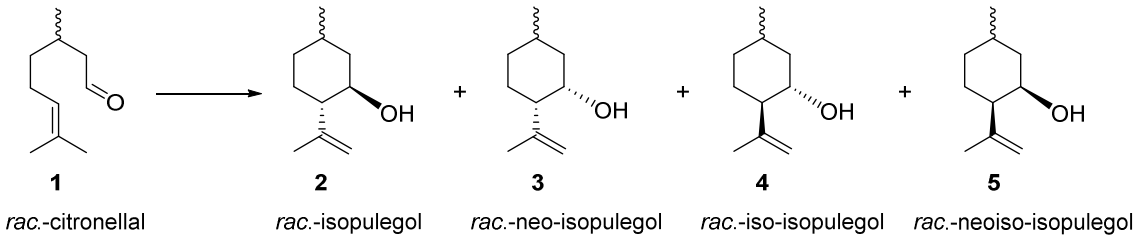

Scheme 3. Isomerization of citronellal to isopulegol.

To study the relative participation of Lewis and Brønsted acid sites in UiO-66, we have performed the citronellal isomerization onto hydrated and dehydrated UiO-66 containing 7% of linker defects. The results are shown in Figure 4.

As it is shown in Fig. 4a, dehydrated UiO-66 shows a significantly higher activity for citronellal isomerization than the hydrated solid: the calculated kinetic rate constants are 0.076 h^{-1} and 0.360 h^{-1} for hydrated and dehydrated UiO-66, respectively (an almost 5-fold increase). This is the exact opposite result that was found for LA esterification, for which dehydration of UiO-66 brings about a decrease of the catalytic activity. As commented above, FTIR spectroscopy of adsorbed CO reveals that hydrated UiO-66 has mainly Brønsted acid sites and virtually no Lewis acid sites (see Fig. 2). Therefore, the lower activity of hydrated versus hydrated UiO-66 indicates that citronellal isomerization is more effectively catalyzed by Lewis acid centers than by Brønsted sites. This is confirmed by the observed diastereoselectivity to isopulegol **2**, which increases from 75% to 86% upon dehydration, reflecting a preferential participation of Lewis acid sites for this reaction. The participation of zirconium Lewis acid sites of UiO-66 in citronellal isomerization was recently rationalized using first-principles kinetic calculations by van Speybroeck and co-workers [9]. Such coordinatively unsaturated Zr sites would be present at defect positions. As expected, the activity increased with the number of linker defects present in the solid catalyst [19]. Note that in hydrated UiO-66, the interaction between citronellal and the zirconium sites of UiO-66 is hindered by the presence of strongly bound water molecules, in such a way that a competition is established between both compounds to coordinate to Zr^{4+} centers, resulting in a slowdown of the reaction.

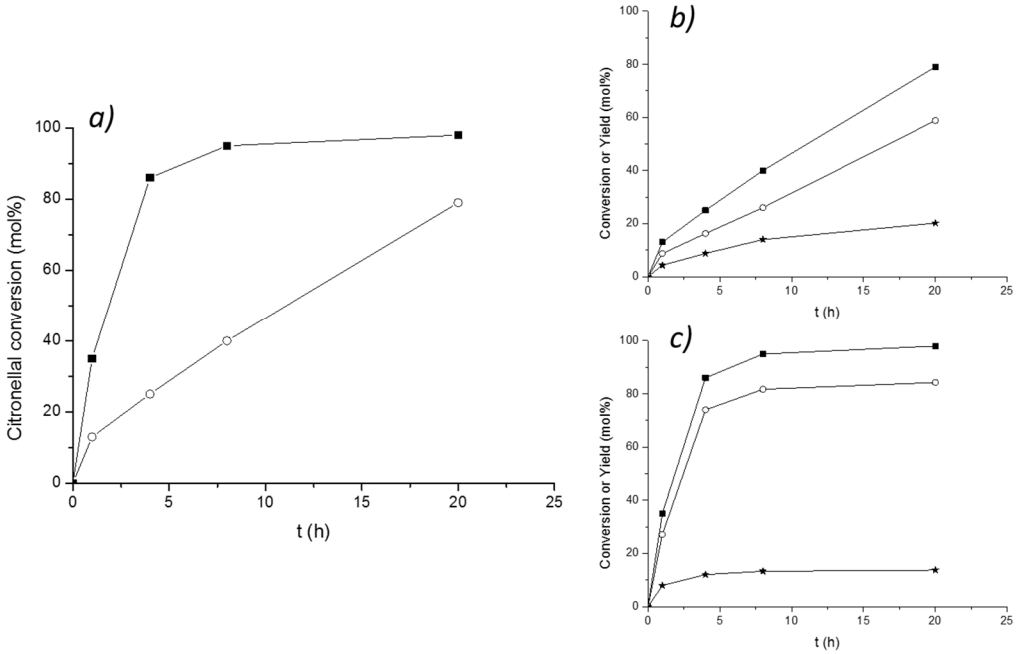

Figure 4. (a) Time-conversion plots of citronellal (**1**) over hydrated (○) and dehydrated (■) UiO-66 (7% defects). Parts (b) and (c) show citronellal conversion (■) and yields to isopulegol **2** (○) and other isopulegols **3**-**5** (*) for hydrated (part b) and dehydrated (part c) UiO-66.

Another reaction that is preferentially catalyzed by Lewis over Brønsted acid sites is the MPV reduction of ketones with secondary alcohols. Indeed, it is generally accepted that this reaction proceeds through a transition state in which the ketone and the alcohol are simultaneously adsorbed onto the coordinatively unsaturated metal sites of the catalyst (acting as a Lewis acid center) and forming a six-membered cyclic structure, as shown in Scheme 4 [54]. Then, a direct hydrogen transfer takes place from the alcohol to the ketone.

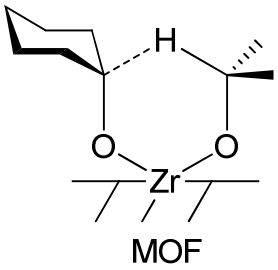

Scheme 4. Six-membered cyclic transition state for the MPV reduction of cyclohexanone with isopropyl alcohol over UiO-66, involving the participation of Zr^{4+} Lewis acid sites.

We have then carried out the MPV reduction of cyclohexanone using isopropanol as the secondary alcohol and using as a catalyst either hydrated or dehydrated UiO-66 containing 7% linker defects. The results are shown in Figure 5.

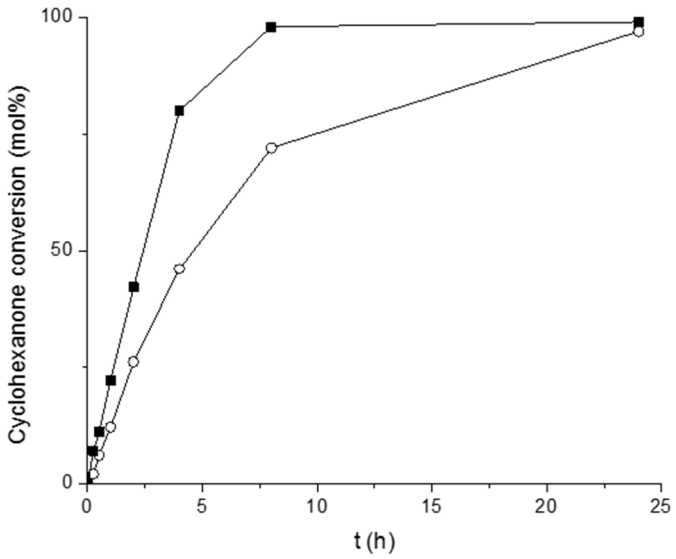

Figure 5. Time-conversion plots of cyclohexanone over hydrated (○) and dehydrated (■) UiO-66 (7% defects).

As it was also the case of citronellal isomerization, dehydration of UiO-66 produces a significant increase of the catalytic activity, passing from a kinetic a rate constant of 0.147 h^{-1} for the hydrated solid, to 0.516 h^{-1} for the dehydrated material, representing a 3.5-fold increase. In line with previous results, the catalytic data for this reaction lend support to the role of the Lewis acid sites associated with linker defects in dehydrated UiO-66 as the main catalytic centers for the MPV reaction. Indeed, we have recently shown that the catalytic activity of various zirconium MOFs in the MPV reduction of cyclohexanone increases in the order MOF-808 > DUT-67 > UiO-66, reflecting the increasing availability of the Zr^{4+} sites as the coordination of the inorganic building units decreases from 12 (UiO-66), to 8 (DUT-67) and to 6 (MOF-808) [20]. Similar results have been reported for the MPV reduction of furfural to furfuryl alcohol [55].

Concluding remarks

Herein we have shown that the hydration degree of UiO-66 is a key factor governing the catalytic properties of UiO-66, in line with previous observations from our lab and by other groups. We have shown that thermal treatment under a vacuum at low temperature (<100ºC) removes physisorbed water molecules trapped inside the MOF pores. However, tightly bound water molecules directly coordinated to zirconium ions at defect positions are still present and requires outgassing at higher temperatures (viz. 200ºC) to be completely removed. These coordinated water molecules are strongly polarized by the Zr^{4+} ions of UiO-66, resulting in the creation of strong Brønsted-induced acid sites. These sites have been revealed by both FTIR spectroscopy of adsorbed CO and by direct pH measurements in methanol.

We have comparatively evaluated the catalytic properties of hydrated and dehydrated UiO-66 in reactions requiring either Brønsted acid sites (esterification of levulinic acid) or Lewis acid sites (citronellal isomerization and MPV reduction of cyclohexanone). We have shown that thermal pre-treatments of the solid under suitable conditions provide a very simple means for controlling the nature of the active sites, shifting the properties of the material from a Brønsted-induced acidity to Lewis acidity. We have shown that this introduces a new dimension in the catalyst engineering that allows us to tune and optimize the performance of the MOF depending on whether the reaction in which it is going to be applied requires Lewis or Brønsted acid sites. So far, this has already been demonstrated for various reactions, including esterification, carbonyl-ene isomerization and MPV reactions over UiO-66 (this work and [32]); acetalization of aldehydes over functionalized MIL-101(Cr) [48]; or the dimerization of isobutene over sulfated MOF-808 [49], to name a few examples.

Experimental details

Synthesis of the MOFs. Different batches of UiO-66 were prepared by the non-modulated synthesis described by Kandiah et al [22]. For this, 750 mg of $ZrCl_4$ and 740 mg of terephthalic acid (UiO-66), or 800 mg of aminoterephthalic acid (UiO-66–NH_2), or 940 mg of nitroterephthalic acid (UiO-66–NO_2) were dissolved in 90 mL of *N, N*-dimethylformamide (DMF) inside a closed round bottom flask and kept at 80ºC for 12 h without stirring, followed by 24 h at 100ºC. The solid thus formed was recovered by centrifugation, washed with fresh DMF (2 x 10 mL) and finally soaked in

dichloromethane for 3 h. The crystallinity of all compounds was confirmed by X-ray diffraction (PhillipsX'Pert, Cu Kα radiation). The number of defects in each sample (see Table 1) was determined by thermogravimetric analysis (Mettler Toledo TGA/SDTA851e, heating rate 10ºC min^{-1} under an air flow), following the method of Valenzano et al. [38]. The corresponding TGA curves, weight losses and determined compositions of these samples are shown in Figure S1 in the Supplementary Material.

Additional batches of UiO-66 and UiO-66 functionalized with sulfonic groups were prepared using a modulated synthesis with acetic acid (samples UiO-66-HAc and UiO-66–SO_3H), following the procedure reported in [19]. Thus, equimolar mixtures of $ZrCl_4$ (3 mmol), the organic ligand (terephthalic or sulfoterephthalic acid) and 10 equivalents of acetic acid were dissolved in DMF (30 mL). The mixture was heated at 120ºC for 21 h, and the powders were collected by centrifugation and washed with fresh DMF (2 x 10 mL) and finally soaked in dichloromethane for 3 h. The crystallinity of all compounds was also confirmed by X-ray diffraction.

All Zr- and Hf-DUT-67 and acid-treated materials mentioned in the text are the same compounds described in [29]. Finally, the Amberlyst-15® catalyst used was a commercial sample from Sigma-Aldrich.

FTIR spectroscopy. The acidity of the UiO-66 type compounds was evaluated using FTIR spectroscopy of adsorbed CO at liquid-nitrogen temperature. IR measurements were performed on a Nikolet i510 FTIR spectrometer at a resolution of 4 cm^{-1}. The solids were prepared in the form of thin self-supported wafers of *ca*. 10 mg cm^{-2} and activated at either 60ºC or 200ºC overnight under vacuum (10^{-3} mbar).

pH measurements. The method used in this work was the same as reported in [48]. Briefly, 6 mg of the MOF (either as-prepared or dehydrated) was dispersed in 24 mL of methanol and kept under stirring for 3 h at room temperature before pH measurements. The amount of MOF used was high enough so the measured pH was independent of the solid content.

Catalytic reactions

Catalyst activation (dehydration). When mentioned in the text, dehydrated MOF catalysts were pre-activated before running the reaction. To do so, the desired amount of fresh MOF was placed directly inside the batch reactor and thermally treated at 150ºC under a vacuum (10^{-3} mbar) overnight. To start the catalytic reaction, the pre-heated solvent and the reagents were directly added to the catalyst inside the batch reactor to avoid exposure to ambient moisture.

Esterification of levulinic acid. 1 mmol of levulinic acid (LA) and 0.6 mL of ethanol (15 mmol) were contacted with the MOF (0.018 mmol of metal) in a batch reactor at 80 °C. The reaction was monitored by GC−MS (Varian 3900) equipped with a BP20(WAX) column (15 m long, i.d. 0.32 mm) and using dodecane as an internal standard. Retention times of the products were compared with those of commercial standards for reference.

Citronellal isomerization. The reaction was performed at 80 °C under a N_2 atmosphere. 60 µl of racemic citronellal and 30 mg of MOF were placed inside a round bottom flask with 0.5 ml of cyclohexane. The reaction was followed by GC-MS equipped with a 30 m long and 0.25 mm i.d. capillary column HP-5 (5% phenylmethylpolysiloxane) and using dodecane as an internal standard. Retention times were compared with those of commercial standards.

Meerwein-Ponndorf-Verley (MPV) reduction of cyclohexanone. In a typical reaction, 10 mg (0.1 mmol) of cyclohexanone were dissolved in 0.5 mL of iPrOH (*ca*. 6.5 eq.). The solution was added to the solid catalyst (14 mol% of metal) under nitrogen atmosphere, and the mixture was transferred into a 2-mL glass batch reactor charged with a magnetic stirrer. The reactor was closed and heated in a metal heating block to 80ºC under stirring. The reaction was followed by GC on an AGILENT 7890A equipped with a FID detector and a DB5 (30 m x 0.25 mm x 0.25 µm) column.

Author Information

Corresponding Authors

* E-mail: fllabres@itq.upv.es, francisco.c.garcia@uv.es

ORCID

Franciscco G. Cirujano: 0000-0002-0159-5777

Francesc X. Llabrés i Xamena: 0000-0002-4238-5784

Notes

The authors declare no competing financial interest.

Biographies

Francesc X. Llabrés i Xamena, or Xesc for short (WoS Researcher ID A-4123-2008) was born in Alaró (Mallorca). He received his PhD in Chemistry in 2000 from the University of the Balearic Islands (Spain) working with Prof. C. Otero in the synthesis and spectroscopic characterization of zeolites. After a 2-years post-doctoral stage at the University of Turin with Prof. A. Zecchina, a short stay as invited researcher at Polimeri Europa (ENI) in Novara, and one year at the University of Padua with Prof. G. Granozzi, he joined the group of Prof. A. Corma at the ITQ in 2004 as a Ramón y Cajal Fellow. In 2010 he was appointed as Tenured Scientist of the Spanish National Research Council

(CSIC) at the ITQ. His current research interests are in the preparation of metal-organic frameworks (MOFs) and the study of their applications, including heterogeneous catalysis. Among other prizes and recognitions, Xesc has been distinguished with the 10th Duran Farrell Award of Technological Research, and the Alpha Gold award of the Spanish Ceramic and Glass Society.

Francisco García Cirujano completed a PhD in Chemistry (2016) at the Institute of Chemical Technology (Valencia, Spain) under the supervision of Dr. Llabrés i Xamena and Prof. Corma. After a postdoctoral stay as a Marie Curie fellow (2017-2019) in the group of Prof. de Vos at KU-Leuven (Belgium), he is now a Junior Leader La Caixa at the University of Valencia. His research on the design and synthesis of high performance metal-organic framework catalysts, aims to achieve environmentally benign processes in the chemical and pharmaceutical industry

Acknowledgments

Financial support by the Spanish Government is acknowledged through projects MAT2017-82288-C2-1-P and the Severo Ochoa program (SEV-2016-0683).

References

1. Corma, A.; Garcia, H.; Llabrés i Xamena, F. X., Engineering Metal Organic Frameworks for Catalysis *Chem. Rev.* **2010**, *110*, 4606-4655.
2. Llabrés i Xamena, F. X.; Gascon, J., *Metal Organic Frameworks as Heterogeneous Catalysts*. first ed.; The Royal Society of Chemistry: Cambridge, 2013.
3. Gascon, J.; Corma, A.; Kapteijn, F.; Llabrés i Xamena, F. X., Metal Organic Framework Catalysis: Quo Vadis? *ACS Catal.* **2014**, *4*, 361-378.
4. Lee, J. Y.; Farha, O. K.; Roberts, J.; Scheidt, K. A.; Nguyen, S. T.; Hupp, J. T., Metal-Organic Framework Materials as Catalysts. *Chem. Soc. Rev.* **2009**, *38*, 1450-1459.
5. Farrusseng, D.; Aguado, S.; Pinel, C., Metal-Organic Frameworks: Opportunities for Catalysis. *Angew. Chem., Int. Ed.* **2009**, *48*, 7502-7513.
6. Zhang, X.; Llabrés i Xamena, F. X.; Corma, A., Gold(III) - Metal Organic Framework Bridges the Gap between Homogeneous and Heterogeneous Gold Catalysts. *J. Catal.* **2009**, *265*, 155-160.
7. Juan-Alcaniz, J.; Ferrando-Soria, J.; Luz, I.; Serra-Crespo, P.; Skupien, E.; Santos, V. P.; Pardo, E.; Llabrés i Xamena, F. X.; Kapteijn, F.; Gascon, J., The Oxamate Route, a Versatile Post-Functionalization for Metal Incorporation in MIL-101(Cr): Catalytic Applications of Cu, Pd, and Au. *J. Catal.* **2013**, *307*, 295-304.
8. Wang, Z. Q.; Cohen, S. M., Postsynthetic Modification of Metal-Organic Frameworks. *Chem. Soc. Rev.* **2009**, *38*, 1315-1329.
9. Vermoortele, F.; Vandichel, M.; Van de Voorde, B.; Ameloot, R.; Waroquier, M.; Van Speybroeck, V.; de Vos, D. E., Electronic Effects of Linker Substitution on Lewis Acid Catalysis with Metal–Organic Frameworks. *Angew. Chem., Int. Ed.* **2012**, *51*, 4887-4890.

10. Vandichel, M.; Vermoortele, F.; Cottenie, S.; de Vos, D. E.; Waroquier, M.; Van Speybroeck, V., Insight in the Activity and Diastereoselectivity of Various Lewis Acid Catalysts for the Citronellal Cyclization. *J. Catal.* **2013**, *305*, 118-129.
11. Cortese, R.; Duca, D., A Dft Study of Irmof-3 Catalysed Knoevenagel Condensation. *Phys. Chem. Chem. Phys.* **2011**, *13*, 15995-16004.
12. Timofeeva, M. N.; Panchenko, V. N.; Jun, J. W.; Hasan, Z.; Matrosova, M. M.; Jhung, S. H., Effects of Linker Substitution on Catalytic Properties of Porous Zirconium Terephthalate UiO-66 in Acetalization of Benzaldehyde with Methanol. *Appl. Catal. A: Gen.* **2014**, *471*, 91-97.
13. Kozachuk, O., et al., Multifunctional, Defect-Engineered Metal–Organic Frameworks with Ruthenium Centers: Sorption and Catalytic Properties. *Angew. Chem., Int. Ed.* **2014**, *53*, 7058-7062.
14. Cirujano, F. G.; Corma, A.; Llabrés i Xamena, F. X., Zirconium-Containing Metal Organic Frameworks as Solid Acid Catalysts for the Esterification of Free Fatty Acids: Synthesis of Biodiesel and Other Compounds of Interest. *Catal. Today* **2015**, *257*, 213-220.
15. Cirujano, F. G.; Corma, A.; Llabrés i Xamena, F. X., Conversion of Levulinic Acid into Chemicals: Synthesis of Biomass Derived Levulinate Esters over Zr-Containing MOFs. *Chem. Eng. Sci.* **2015**, *124*, 52-60.
16. Rechac, V. L.; Cirujano, F. G.; Corma, A.; Llabrés i Xamena, F. X., Diastereoselective Synthesis of Pyranoquinolines on Zirconium-Containing UiO-66 Metal-Organic Frameworks. *Eur. J. Inorg. Chem.* **2016**, *2016*, 4512-4516.
17. Kim, J.; Kim, S.-N.; Jang, H.-G.; Seo, G.; Ahn, W.-S., CO_2 Cycloaddition of Styrene Oxide over MOF Catalysts. *Appl. Catal. A: Gen.* **2013**, *453*, 175-180.
18. Vermoortele, F.; Ameloot, R.; Vimont, A.; Serre, C.; de Vos, D. E., An Amino-Modified Zr-Terephthalate Metal–Organic Framework as an Acid–Base Catalyst for Cross-Aldol Condensation. *Chem. Commun.* **2011**, *47*, 1521-1523.
19. Vermoortele, F., et al., Synthesis Modulation as a Tool to Increase the Catalytic Activity of Metal-Organic Frameworks: The Unique Case of UiO-66(Zr). *J. Am. Chem. Soc.* **2013**, *135*, 11465-11468.
20. Mautschke, H.-H.; Drache, F.; Senkovska, I.; Kaskel, S.; Llabrés i Xamena, F. X., Catalytic Properties of Pristine and Defect-Engineered Zr-MOF-808 Metal Organic Frameworks. *Catal. Sci. Technol.* **2018**, *8*, 3610-3616.
21. Dissegna, S.; Hardian, R.; Epp, K.; Kieslich, G.; Coulet, M. V.; Llewellyn, P. L.; Fischer, R. A., Using Water Adsorption Measurements to Access the Chemistry of Defects in the Metal–Organic Framework UiO-66. *CrystEngComm* **2017**, *19*, 4137-4141.
22. Kandiah, M.; Nilsen, M. H.; Usseglio, S.; Jakobsen, S.; Olsbye, U.; Tilset, M.; Larabi, C.; Quadrelli, E. A.; Bonino, F.; Lillerud, K. P., Synthesis and Stability of Tagged UiO-66 Zr-MOFs. *Chem. Mater.* **2010**, *22*, 6632-6640.
23. Nandiwale, K. Y.; Bokade, V. V., Esterification of Renewable Levulinic Acid to N-Butyl Levulinate over Modified H-ZSM-5. *Chem. Eng. Technol.* **2015**, *38*, 246-252.
24. Dharne, S.; Bokade, V. V., Esterification of Levulinic Acid to N-Butyl Levulinate over Heteropolyacid Supported on Acid-Treated Clay. *J. Nat. Gas Chem.* **2011**, *20*, 18-24.
25. Saravanan, K.; Tyagia, B.; Shukla, R. S.; Bajaj, H. C., Esterification of Palmitic Acid with Methanol over Template-Assisted Mesoporous Sulfated Zirconia Solid Acid Catalyst. *Appl. Catal. B: Environm.* **2015**, *172-173*, 108-115.
26. Zatta, L.; Ramos, L. P.; Wypych, F., Acid-Activated Montmorillonites as Heterogeneous Catalysts for the Esterification of Lauric Acid Acid with Methanol. *Appl. Clay Sci.* **2013**, *80-81*, 236-244.
27. Goesten, M. G.; Juan-Alcaniz, J.; Ramos-Fernandez, E. V.; Gupta, K. B. S. S.; Stavitski, E.; van Bekkum, H.; Gascon, J.; Kapteijn, F., Sulfation of Metal–Organic Frameworks: Opportunities for Acid Catalysis and Proton Conductivity. *J. Catal.* **2011**, *281*, 177-187.
28. Jiang, J.; Gándara, F.; Zhang, Y.-B.; Na, K.; Yaghi, O. M.; Klemperer, W. G., Superacidity in Sulfated Metal−Organic Framework-808. *J. Am. Chem. Soc.* **2014**, *136*, 12844-12847.

29. Drache, F.; Cirujano, F. G.; Nguyen, K. D.; Bon, V.; Senkovska, I.; Llabrés i Xamena, F. X.; Kaskel, S., Anion Exchange and Catalytic Functionalization of the Zirconium-Based Metal−Organic Framework DUT-67. *Cryst. Growth Des.* **2018**, *18*, 5492-5500.
30. Alaerts, L.; Seguin, E.; Poelman, H.; Thibault-Starzyk, F.; Jacobs, P. A.; De Vos, D. E., Probing the Lewis Acidity and Catalytic Activity of the Metal-Organic Framework $Cu_3(BTC)_2$ (BTC = Benzene-1,3,5-Tricarboxylate). *Chem. Eur. J* **2006**, *12*, 7353-7363.
31. Cirujano, F. G.; Llabres i Xamena, F. X.; Corma, A., Mofs as Multifunctional Catalysts: One-Pot Synthesis of Menthol from Citronellal over a Bifunctional MIL-101 Catalyst. *Dalton Trans.* **2012**, *41*, 4249-4254.
32. Caratelli, C.; Hajek, J.; Cirujano, F. G.; Waroquier, M.; Llabrés i Xamena, F. X.; Van Speybroeck, V., Nature of Active Sites on UiO-66 and Beneficial Influence of Water in the Catalysis of Fischer Esterification. *J. Catal.* **2017**, *352*, 401-414.
33. Ghosh, P.; Colón, Y. J.; Snurr, R. Q., Water Adsorption in UiO-66: The Importance of Defects. *Chem. Commun.* **2014**, *50*, 11329-11331.
34. Schoenecker, P. M.; Carson, C. G.; Jasuja, H.; Flemming, C. J. J.; Walton, K. S., Effect of Water Adsorption on Retention of Structure and Surface Area of Metal−Organic Frameworks. *Ind. Eng. Chem. Res.* **2012**, *51*, 6513-6519.
35. Zecchina, A.; Otero Arean, C., Diatomic Molecular Probes for Mid-IR Studies of Zeolites. *Chem. Soc. Rev.* **1996**, *25*, 187-197.
36. Zaera, F., New Advances in the Use of Infrared Absorption Spectroscopy for the Characterization of Heterogeneous Catalytic Reactions. *Chem. Soc. Rev.* **2014**, *43*, 7624-7663.
37. Bonino, F.; Lamberti, C.; Chavan, S.; Vitillo, J. G.; Bordiga, S., Characterization of Mofs. 1. Combined Vibrational and Electronic Spectroscopies. In *Metal Organic Frameworks as Heterogeneous Catalysts*, Llabrés i Xamena, F. X.; Gascón, J., Eds. The Royal Society of Chemistry: Cambridge, 2013; pp 76-142.
38. Valenzano, L.; Civalleri, B.; Chavan, S.; Bordiga, S.; Nilsen, M. H.; Jakobsen, S.; Lillerud, K. P.; Lamberti, C., Disclosing the Complex Structure of UiO-66 Metal Organic Framework: A Synergic Combination of Experiment and Theory. *Chem. Mater.* **2011**, *23*, 1700-1718.
39. Shearer, G. C.; Forselv, S.; Chavan, S.; Bordiga, S.; Mathisen, K.; Bjorgen, M.; Svelle, S.; Lillerud, K. P., In Situ Infrared Spectroscopic and Gravimetric Characterisation of the Solvent Removal and Dehydroxylation of the Metal Organic Frameworks UiO-66 and UiO-67. *Top. Catal.* **2013**, *56*, 770-782.
40. Wiersum, A. D., et al., An Evaluation of UiO-66 for Gas-Based Applications. *Chem. Asian. J.* **2011**, *6*, 3270-3280.
41. Driscoll, D. M.; Troya, D.; Usov, P. M.; Maynes, A. J.; Morris, A. J.; Morris, J. R., Geometry and Energetics of Co Adsorption on Hydroxylated UiO-66. *Phys. Chem. Chem. Phys.* **2019**, *21*, 5078-5085.
42. Driscoll, D. M.; Troya, D.; Usov, P. M.; Maynes, A. J.; Morris, A. J.; Morris, J. R., Characterization of Undercoordinated Zr Defect Sites in UiO-66 with Vibrational Spectroscopy of Adsorbed Co. *J. Phys. Chem. C* **2018**, *118*, 14582-14589.
43. Chakarova, K.; Strauss, I.; Mihaylov, M.; Drenchev, N.; Hadjiivanov, K., Evolution of Acid and Basic Sites in Uio-66 and UiO-66-NH_2 Metal-Organic Frameworks: FTIR Study by Probe Molecules. *Microporous Mesoporous Mater.* **2019**, *281*, 110-122.
44. Vimont, A.; Goupil, J. M.; Lavalley, J. C.; Daturi, M.; Surble, S.; Serre, C.; Millange, F.; Ferey, G.; Audebrand, N., Investigation of Acid Sites in a Zeotypic Giant Pores Chromium(III) Carboxylate. *J. Am. Chem. Soc.* **2006**, *128*, 3218-3227.
45. Vimont, A.; Leclerc, H.; Mauge, F.; Daturi, M.; Lavalley, J. C.; Surble, S.; Serre, C.; Ferey, G., Creation of Controlled Bronsted Acidity on a Zeotypic Mesoporous Chromium(III) Carboxylate by Grafting Water and Alcohol Molecules. *J. Phys. Chem. C* **2007**, *111*, 383-388.
46. Volkringer, C.; Leclerc, H.; Lavalley, J. C.; Loiseau, T.; Ferey, G.; Daturi, M.; Vimont, A., Infrared Spectroscopy Investigation of the Acid Sites in the Metal-Organic Framework Aluminum Trimesate MIL-100(Al). *J. Phys. Chem. C* **2012**, *116*, 5710-5719.

47. Walker, J. D.; Newman, M. C.; Enache, M., *Fundamental Qsars for Metal Ions*; CRC Press, 2013.
48. Herbst, A.; Khutia, A.; Janiak, C., Brønsted Instead of Lewis Acidity in Functionalized MIL-101Cr MOFs for Efficient Heterogeneous (Nano-MOF) Catalysis in the Condensation Reaction of Aldehydes with Alcohols. *Inorg. Chem.* **2014**, *53*, 7319-7333.
49. Trickett, C. A., et al., Identification of the Strong Brønsted Acid Site in a Metal–Organic Framework Solid Acid Catalyst. *Nature Chem.* **2019**, *11*, 170-176.
50. Wulfsberg, G., *Inorganic Chemistry*; University Science Books, 2000.
51. Jiang, J.; Yaghi, O. M., Brønsted Acidity in Metal−Organic Frameworks. *Chem. Rev.* **2015**, *115*, 6966-6997.
52. Klet, R. C.; Liu, Y.; Wang, T. C.; Hupp, J. T.; Farha, O. K., Evaluation of Brønsted Acidity and Proton Topology in Zr- and Hf-Based Metal–Organic Frameworks Using Potentiometric Acid–Base Titration. *J. Mater. Chem. A* **2016**, *4*, 1479-1485.
53. Reddy, C. R.; Vijayakumar, B.; Iyengar, P.; Nagendrappa, G.; Prakash, B. S. J., Synthesis of Phenylacetates Using Aluminium-Exchanged Montmorillonite Clay Catalyst. *J. Mol. Catal. A-Chem.* **2004**, *223*, 117-122.
54. de Graauw, C. F.; Peters, J. A.; Van Bekkum, H.; Huskens, J., Meerwein-Ponndorf-Verley Reductions and Oppenauer Oxidations: An Integrated Approach. *Synthesis* **1994**, *10*, 1007-1017.
55. Valekar, A. H.; Lee, M.; Yoon, J. W.; Kwak, J.; Hong, D. Y.; Oh, K. R.; Cha, G. Y.; Kwon, Y. U.; Jung, J.; Chang, J. S.; Hwang, Y. K., Catalytic Transfer Hydrogenation of Furfural to Furfuryl Alcohol under Mild Conditions over Zr-MOFs: Exploring the Role of Metal Node Coordination and Modification. *ACS Catal.* **2020**, *10*, 3720-3732.